Proceedings of the 17th World Congress
The International Federation of Automatic Control
Seoul, Korea, July 6-11, 2008

On Control of Planar Switched Reluctance Motor

Jin Ming Yang*, Qing Zhong*, Norbert C. Cheung and Shi Wei Zhao****

**Electric Power College, South China University of Technology, Guangzhou, China (e-mail: jmyang@scut.edu.cn).*
*** Department of Electrical Engineering, Hong Kong Polytechnic University, Hunghom, Kowloon, Hong Kong SAR, China (e-mail: eencheun@polyu.edu.hk).*

Abstract: By using the energy dissipation theory and the property of the switched reluctance motor, this paper presents a nonlinear controller for the planar switched reluctance motors (PSRM). Based on the fact that the electrical time constant is much smaller than the mechanical time constant, the whole PSRM driving system is treated as a two-time-scale system and can be decomposed into two subsystems (electrical and mechanical) that are negative feedback interconnection. The controllers are designed for two subsystems respectively to ensure that they are passive. In view of the fact that the system made of two passive subsystem connected through negative feedback is still passive. Therefore, the stability of PSRM driving system is ensured in large scale. This control strategy possesses a simple structure and can be implemented easily. The experimental results show that the proposed control is effective for the position control of PSRM.

1. INTRODUCTION

Modern industrial applications often require two-directional (2-D) motions. Traditional X-Y tables using rotary motors with mechanical transmissions stacked on top of each other have high cost, reduced accuracy, complex mechanical structure, and frequent maintenance. Planar motors have drawn much research attention over the past decade. The planar motors drive directly the platform move in 2-D. It overcomes many shortcomings in rotary motor. PSRM has also the properties of switched reluctance motors such as simple structure, ruggedness and reliability in harsh environments. These advantages make PSRM an alternative choice for direct-drive application (Pan (2005) and (2006)).

The flux link is the nonlinear function of the position and the current for switched reluctance motor. And this kind of motor possesses inherent thrust ripple made from the slot structure. The control of speed and position is difficult. These limit it application in precise motion. The proposed several methods to overcome the above problems mostly existed in rotary switched reluctance motor. The nonlinear control method is applied in PSRM in many examples. The method feedback linearization controller is designed to improve the dynamic property in position and speed tracking (Panda (1996)). And the adaptive controller is applied to estimate the parameters (Milman (1999)). There is also a simple lookup tables for linear switched reluctance motor (Gan (2003)). The iterative learning control is applied to realize the indirect torque control (Sahoo (2005)). The article (Xia (2006)) adopted the RBF neural network to control the speed of switched reluctance motor. The article (Pan (2006)) applied auto-disturbance rejection controller in the PSRM. All the above methods only stress on the control strategy themselves. The structural property of switched reluctance motor is not referred.

In this paper, a nonlinear feedback controller, which effectively combines the natural energy dissipation properties of PSRM, is proposed. The passivity-based controllers have been applied successfully in rotary switched reluctance motor and switched reluctance gripper which property is similar to that of the switched reluctance motor (Xia (2006), Espinosa-Pérez (2004), Yang (2004) and Chan (2005)). In these methods, PSRM was treated as a whole plant to design their controllers. Following the fact that the electrical time constant is much smaller than the mechanical time constant, the whole PSRM driving system is viewed as a two-time-scale system and can be decomposed into two subsystems (electrical and mechanical) that are negative feedback interconnection. The controllers are designed for two subsystems respectively. The controllers are designed to achieve the required properties by damp injection and ensure each subsystem is stable. In view of the fact that the system made of two passive subsystem connected through negative feedback is still passive. The stability of PSRM driving system is ensured in large scale. This control strategy possesses a simple structure and can be implemented easily.

The organization of this paper is as follows. Construction and modelling of the PSRM and controller design are given in section 2 and 3; experimental results are presented in section 4. Finally, the conclusions are described in section 5.

2. CONSTRUCTION AND MODEL OF PSRM

2.1 Configuration of PSRM

In this paper, the proposed PSRM design schematic is shown in figure 1. The PSRM derived from the linear switched reluctance motor and consists of mover and stator. The mover has two sets of three-phase winding. The six windings have the same dimension and the sets are mounted vertically to each other as shown in figure 2. The mover is supported by two sets of sliding blocks which can move in X-axis and Y-axis direction respectively. The stator contains multiple laminated silicon-steel blocks held together by epoxy, a rigid aluminium based plate to support them, and sliding supports to hold the platform and maintain the air-gap. The structure of stator is constructed from the combinations of magnetic blocks and extended by means of "building blocks" as shown in Figure 3. Two 0.5um resolution linear optical encoders are integrated in the PSRM system to provide the information of position.

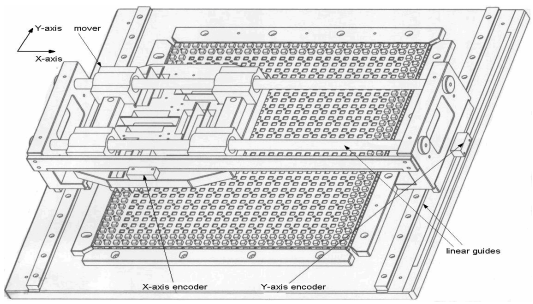

Fig. 1 The planar switched reluctance motor.

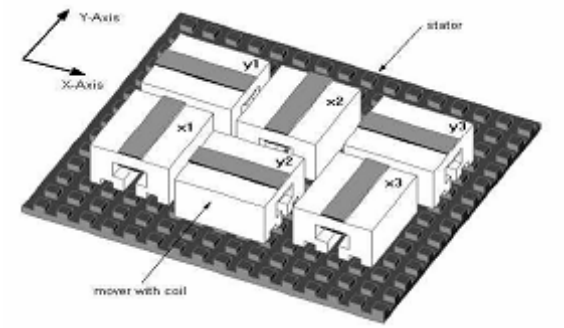

Fig. 2 Mover Schematic of the PSRM.

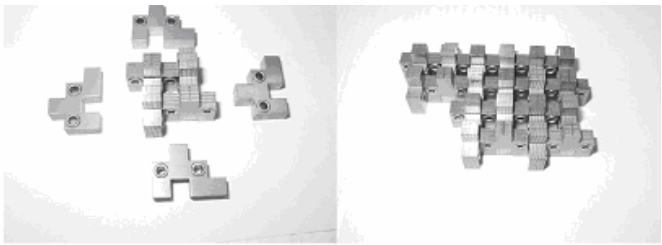

(a) (b)

Fig. 3 Construction of the stator base.
(a) Individual laminated steel blocks making up the stator and
(b) grouping the blocks together to form the base of the stator.

2.2 Modelling of PSRM

Because the special arrangement is applied to make the mover windings flux-decoupled between adjacent windings, the mutual inductance is approaching to zero. The PSRM can be taken as two independent linear switched reluctance motors. The control of PSRM can also be decomposed into the control of two linear switched reluctance motors. The model of PSRM in one direction motion is given as follows.

$$u_j = r_j i_j + \frac{\partial \lambda_j}{\partial i_j}\frac{di_j}{dt} + \frac{\partial \lambda_j}{\partial x}\frac{dx}{dt}, j = a,b,c. \quad (1)$$

$$M\frac{d^2x}{dt^2} = f_e - B\frac{dx}{dt} - f_l. \quad (2)$$

u_j is the voltage applied to the terminals of phase j, i_j is the current of phase j, r_j is the winding resistance and λ_j is the phase flux linkage of phase j, L_i is the phase inductance, x is the displacement, M and B are the mass and friction constant respectively, f_l is the external load force. f_e is the generated electromagnetic force.

$$f_j(x,i_j) = \frac{1}{2}\frac{dL_j}{dx}i_j^2, j = a,b,c. \quad (3)$$

$$f_e = \sum_{j=a}^{c} f_j. \quad (4)$$

2.3 Decomposition of PSRM

The PSRM possesses the two-time-scale characteristics and can be decomposed into an electrical subsystem (Σ_e) and a mechanical subsystem (Σ_m). The linkage of these two subsystems is nonlinear negative feedback as shown in figure 4.

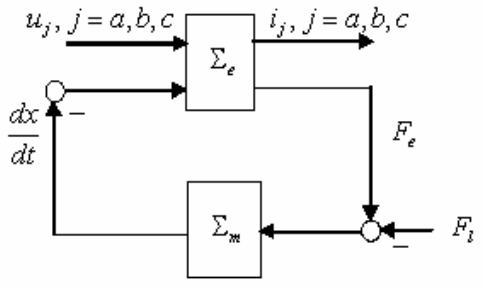

Fig. 4 Passive subsystem decomposition.

Σ_e and Σ_m are passive mapping, i.e.

$$\Sigma_e : \begin{bmatrix} u_j \\ -\frac{dx}{dt} \end{bmatrix} \mapsto \begin{bmatrix} i_j \\ f_e \end{bmatrix}, \Sigma_m : (f_e - f_l) \mapsto \frac{dx}{dt}.$$

3. PBC DESIGN

3.1 The PBC for electrical subsystem

The electrical loop is a third-order subsystem. Taking the $z_1 = [i_a \quad i_b \quad i_c]^T$ as the state vector of Σ_e. The dynamic property of Σ_e can be described as follows

$$D\dot{z}_1 = [-J(z_2) - R]z_1 + gu_1 \tag{5}$$

where g is the input vector, u_1 is the control signal. $J(z_2)$ and R are the structure matrices. The matrix R is a strictly positive definite symmetric matrix and corresponds to the energy dissipating of the model. D is an inductance matrix. $J(z_2)$ is the rate of inductance matrix and relative to the state z_2 in the mechanical subsystem.

$$J(z_2) = \begin{bmatrix} \frac{\partial L_1}{\partial x}\frac{dx}{dt} & & \\ & \frac{\partial L_2}{\partial x}\frac{dx}{dt} & \\ & & \frac{\partial L_2}{\partial x}\frac{dx}{dt} \end{bmatrix}, \quad R = \begin{bmatrix} r_a & & \\ & r_b & \\ & & r_c \end{bmatrix},$$

$$D = \begin{bmatrix} L_1 & & \\ & L_2 & \\ & & L_3 \end{bmatrix} \text{ and } g = [1,1,1]^T.$$

Define the state error as $e = z_1 - z_d$ where z_d is the reference state vector which defines the desired system performance. Substituting the state error into equation (5) yields the model of the state error as

$$D\dot{e} + Re = -D\dot{z}_d - Rz_d - J(z_2)z_1 + gu = \Phi \tag{6}$$

Choosing the energy function of state error for Σ_e as

$$H(e) = \frac{1}{2}e^T De. \tag{7}$$

Differentiating the $H(e)$ to time along the state error equation (6), we get

$$\dot{H}(e) = -e^T Re + e^T\Phi + \frac{1}{2}e^T\dot{D}e. \tag{8}$$

By keeping $\Phi + \frac{1}{2}\dot{D}e = 0$, we get

$$\dot{H}(e) = -e^T Re. \tag{9}$$

In equation (9), R is a strictly positive definite matrix and $\dot{H}(e)$ is a negative definite matrix, hence the state error subsystem (6) is strictly passive and stable.

Because $\Phi + \frac{1}{2}\dot{D}e = 0$ is hard to precisely implement, the control algorithm can be designed by using $\Phi + \frac{1}{2}\dot{D}e \le 0$. The stability can also be ensured. Besides, damping injection could be applied for enhancing the rate of convergence of the state error as

$$\Phi + \frac{1}{2}\dot{D}e = -Ke. \tag{10}$$

where $K = diag\{k_1, k_2, k_3\}$ is a positive definite matrix and the parameters of the matrix are adjustable.

$$\dot{H}(e) = -e^T(R + K)e. \tag{11}$$

Therefore, the control law for Σ_e is designed as

$$\begin{aligned} u_1 &= L_1\dot{z}_{d1} + r_a z_{d1} + \frac{\partial L_1}{\partial x}\frac{dx}{dt}z_{11} - \frac{1}{2}\frac{\partial L_1}{\partial x}\frac{dx}{dt}e_1 - k_1 e_1 \\ u_2 &= L_2\dot{z}_{d2} + r_b z_{d2} + \frac{\partial L_2}{\partial x}\frac{dx}{dt}z_{12} - \frac{1}{2}\frac{\partial L_2}{\partial x}\frac{dx}{dt}e_2 - k_2 e_2 \\ u_3 &= L_3\dot{z}_{d3} + r_c z_{d3} + \frac{\partial L_3}{\partial x}\frac{dx}{dt}z_{13} - \frac{1}{2}\frac{\partial L_3}{\partial x}\frac{dx}{dt}e_3 - k_3 e_3 \end{aligned} \tag{12}$$

3.2 The PBC for mechanical subsystem

Taking $z_2 = v$ as the state variable for Σ_m. The dynamic property of Σ_m can be described as follow.

$$M\dot{z}_2 = -Bz_2 + f_e - f_l. \tag{13}$$

Define the state error as $e_4 = z_2 - z_{d2}$ where z_{d2} is the reference state vector which defines the desired system performance. The state error equation of Σ_m can been rewritten as

$$M\dot{e}_4 = -Be_4 - M\dot{z}_{d2} + Bz_{d2} + f_e - f_l. \tag{14}$$

Because the natural damp of Σ_m is much small. The dynamic performance is also improved by injecting damp. The control law is designed as

$$f_e = M\dot{z}_{d2} + Bz_{d2} - f_l - k_4 e_4 \tag{15}$$

where $-k_4 e_4$ is the term of injecting damp.

3.3 The speed tracking and the analyse of PSRM

It is necessary to perform current commutation with position for a proper PSRM operation. Therefore, a motor winding excitation scheme is developed. Generally, a motor winding excitation scheme can be considered as a Force Distribution Function (FDF) and an approximated function of inductance change rate. The diagram of a motor winding excitation scheme can be represented as in figure 5. The FDF is used to compute the force for each phase according to the position and the direction. The approximated function of inductance change rate is used to compute the phase current according to the command force of phase and the position. Some methods have been proposed for the approximated function of inductance change rate.

Taking the z_{d2} as the desired constant speed v^*. The desired thrust can be calculate from (15) as

$$f_e^* = Bz_{d2} - f_l - k_4 e_4 . \qquad (16)$$

This f_e^* is taken as the desired force. And the z_d can be calculate. So the track to the desired speed can been achieved.

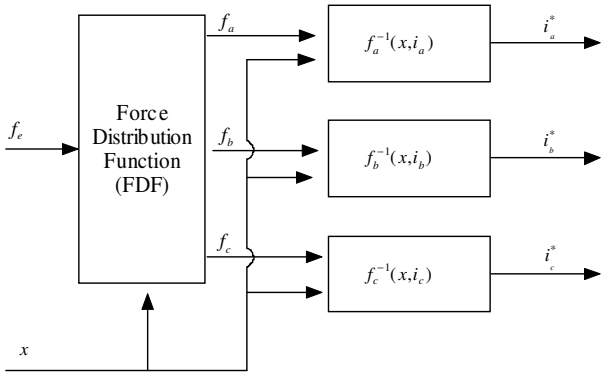

Fig.5 The diagram of a motor winding excitation scheme.

Form figure 4, the reference current for each phase is calculated by using the desired force f_e^* according to the required performances of Σ_m

$$i_{jd} = \sqrt{2f_e^* \Big/ \frac{dL_j}{dx}} \qquad (17)$$

where $\frac{dL_j}{dx}$ is obtained by using look-up table.

Define the energy function of state error for he whole PSRM system as

$$H^*(e) = \frac{1}{2} e^T De + \frac{1}{2} e_4^T M e_4 . \qquad (18)$$

Differentiating the $H^*(e)$ to time along the Σ_m and Σ_e, and substituting the proposed controller (12) and (15), the stability of PSRM can be proved and the state error would exponentially converge to zero.

4. EXPERIMENTAL RESULTS

The experimental Schematic is shown in figure 6. The host PC is a Pentium 4 computer that is used to download the target code into a dSPACE DS1104 DSP motion controller card and supports an interface to adjust the system parameters on real-time. The control algorithm is developed under the environment of MATLAB/SIMULINK. All control functions are implemented and state variables are sampled by the DS1104 card, which is plugged into a PCI bus of the host PC. The driver consists of three asymmetric bridge MOSFET inverters with DC voltage supplier corresponding to the three winding respectively.

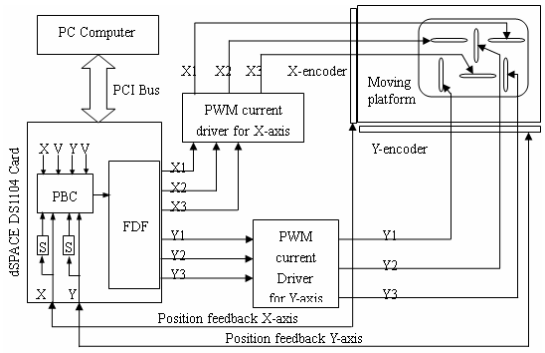

Fig. 6 Experimental setup of the driving system.

The proposed control algorithm is simulated for its effectiveness with the MATLAB software. The parameters of PSRM are listed in Table 1. The applied FDF is listed in Table 2.

Table 1 Parameters of planar motor

Parameter	Value
Pole pitch	6 mm
Pole width	6 mm
Pole slot	6 mm
Air gap	0.55mm
Number of turns per phase	160N
Rated power	120W
Phase reluctance	1.5Ω
Size of base plate	450 mm ×450mm
Travel distance	300 mm ×300mm
Mover mass(X)	8.75Kg
Mover mass(Y)	15Kg

Table 2 Force distribution function (FDF) scheme

region	Position (mm)	+ Force command	-Force command
1	0-2	B	C, A
2	2-4	B, C	A
3	4-6	C	A, B
4	6-8	C, A	B
5	8-10	A	B, C
6	10-12	B, A	C

The square waveform is adopted in the experiment. To avoid undesired oscillation response, instead of using the pure square waveform to test the tracking performance, a quasi third-order S-function signal is used. The frequency of square waveform signal is 0.5Hz and the amplitude is 20mm.

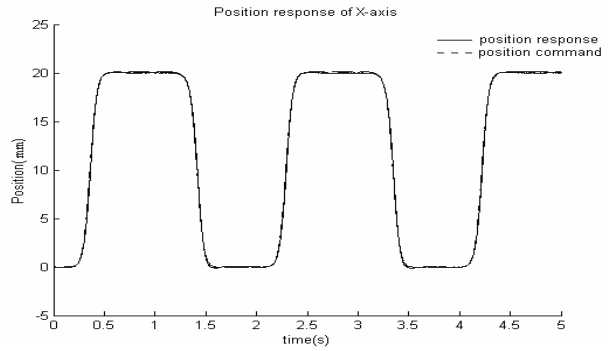

(a) X-axis

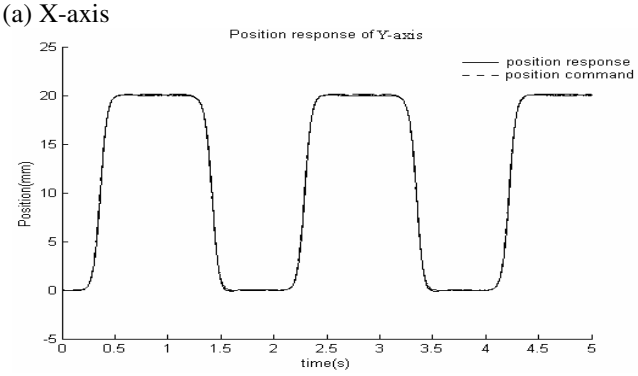

(b) Y-axis

Fig. 7 The experimental curve of position response.

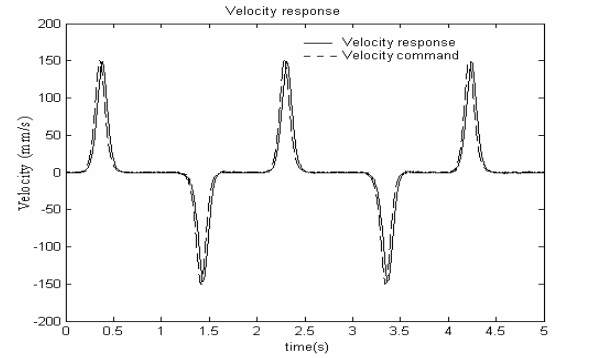

(a) X-axis

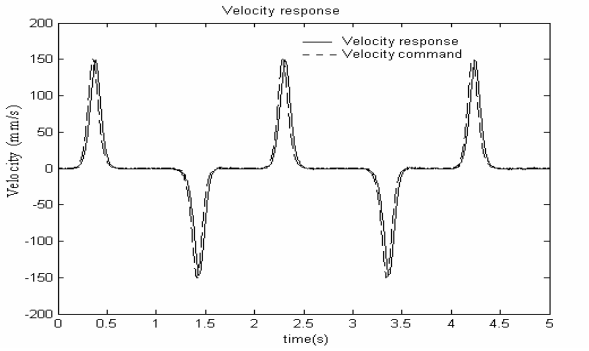

(b) Y-axis

Fig. 8 The experimental curve of speed response.

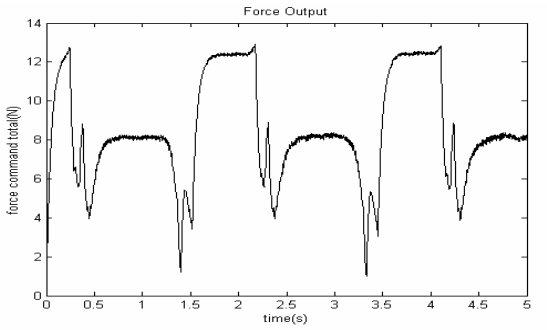

Fig. 9 Command signal of force.

Figure 7 shows the process of position response in X-axis and Y-axis respectively. Figure 8 shows the process of speed response. Figure 9 shows the corresponding the command of force distribution function during the speed response. The experimental results demonstrate that the proposed algorithm not only make the PSRM driving system possess high position precision and speed precision but also equip with perfect dynamics.

5. CONCLUSIONS

The PSRM driving system is decomposed into an electrical subsystem and a mechanical subsystem. The order of the decomposed system is reduced. The PBCs are designed for electrical subsystem and mechanical subsystem respectively based on the properties of the two-time-scale and passivity. This simplifies the controller structure and makes controller design tractable. The strict passivity of the two subsystems and their negative feedback interconnection ensure the stability of the proposed controller for the whole driving system. The experimental results show that the proposed method is effective and can be realized easily.

ACKNOWLEDGMENT

The authors would like to thank the National Natural Science Foundation of China (60674099) and the University Grants Council for the funding support of this research work through project code: PolyU 5224/04E.

REFERENCES

Pan, J.F., N.C. Cheung and J.M. Yang (2005). High-precision position control of a novel planar switched reluctance motor. *IEEE Trans. Ind. Applicat.*, **52(6)**, 1644-1652.

Pan, J.F., N.C. Cheung, W.C. Gan and S.W. Zhao (2006). A novel planar switched reluctance motors for industrial application. *IEEE Trans. on Magnetics*, **42(10)**, 2836-2839.

Pan, J.F., N.C. Cheung and J.M. Yang (2006). Auto-disturbance rejection controller for novel planar switched reluctance motor. *IEE Pro.-Electr. Power Appl.*, **153(2)**, 307-316.

Panda, S.K. and P.K. Dash (1996). Application of nonlinear control to switched reluctance motors: a feedback linearization approach. *IEE Pro.-Electr. Power Appl.*, **143,** 371-379.

Milman, R. and S.A. Bortoff (1999). Observer-based adaptive control of a variable reluctance motor: experimental results. *IEEE Trans. Contr. System Tech.*, **7,** 613-621.

Gan, W.C., N.C. Cheung and L. Qiu (2003). Position control of linear switched reluctance motors for high precision applications. *IEEE Trans. Ind. Applicat.*, **39(5),** 1350-1362.

Sahoo, S.K., S.K. Panda and J. Xu (2005). Indirect Torque Control of Switched Reluctance Motors Using Iterative Learning Control. *IEEE Trans. on Power Electronics*, 20(1), 200-208.

Xia, C., Z. Chen and M. Xue (2006). Adaptive PWM Speed Control for Switched Reluctance Motors Based on RBF Neural Network. *Proceedings of the 6th World Congress on Intelligent Control and Automation,* June 21-23, 2006, Dalian, China.

Espinosa-Pérez, G., P. Maya-Ortiz, M. Velasco-Villa and H. Sira-Ramíez (2004). Passivity-based control of switched reluctance motors with nonlinear magnetic circuits. *IEEE Trans. Contr. System Tech.*, **12,** 439-448.

Yang, J.M., X. Jin, J. Wu, N.C. Cheung and K.K. Chan (2004). Passivity-based control incorporating trajectory planning for a variable-reluctance finger gripper. *Proc. Instn Mech. Engrs Part I: J. Systems and Control Engineering*, **218,** 99-109.

Chan, K.K., J.M. Yang and N.C. Cheung (2005). Passivity-based control for flux regulation in a variable reluctance finger gripper. *IEE Pro.-Electr. Power Appl.*, **152,** 686-694.

Ilic'-Spong, M., Marino, R., Peresada, S. M. and Taylor, D. G.: 'Feedback linearizing control of switched reluctance motors', IEEE Trans. Automat. Contr., 1987, **AC-32**, pp. 371-379